

Journal Pre-proof

Thermal hysteresis activity of antifreeze proteins: A model based on fractional statistics theory of adsorption

J.I. Lopez Ortiz, E. Quiroga, C.F. Nambuena, J.L. Riccardo,
A.J. Ramirez-Pastor



PII: S0378-4371(21)00319-8
DOI: <https://doi.org/10.1016/j.physa.2021.126046>
Reference: PHYSA 126046

To appear in: *Physica A*

Received date: 21 May 2020
Revised date: 24 October 2020

Please cite this article as: J.I.L. Ortiz, E. Quiroga, C.F. Nambuena et al., Thermal hysteresis activity of antifreeze proteins: A model based on fractional statistics theory of adsorption, *Physica A* (2021), doi: <https://doi.org/10.1016/j.physa.2021.126046>.

This is a PDF file of an article that has undergone enhancements after acceptance, such as the addition of a cover page and metadata, and formatting for readability, but it is not yet the definitive version of record. This version will undergo additional copyediting, typesetting and review before it is published in its final form, but we are providing this version to give early visibility of the article. Please note that, during the production process, errors may be discovered which could affect the content, and all legal disclaimers that apply to the journal pertain.

© 2021 Elsevier B.V. All rights reserved.

Thermal hysteresis activity of antifreeze proteins: a model based on fractional statistics theory of adsorption

J. I. Lopez Ortiz ^a, E. Quiroga ^c, C. F. Narambuena ^{a,b},
J. L. Riccardo ^a, A. J. Ramirez-Pastor ^{a,1}

^a*Departamento de Física, Instituto de Física Aplicada, Universidad Nacional de San Luis-CONICET, Ejército de Los Andes 950, D5700BWS San Luis, Argentina*

^b*Universidad Tecnológica Nacional, Facultad Regional San Rafael, CONICET, Gral. Urquiza 314, 5600, San Rafael, Mendoza, Argentina*

^c*Laboratorio de Membranas y Biomateriales, Instituto de Física Aplicada, Universidad Nacional de San Luis-CONICET, Ejército de Los Andes 950, D5700BWS San Luis, Argentina*

Abstract

Antifreeze proteins (AFPs) adsorb to the surface of embryonic ice crystals to prevent their growth. The protein-ice adsorption lowers the freezing point of the solution. Then, a thermal hysteresis can be defined as the difference between the melting and freezing temperatures. This quantity is a measure of the antifreeze protein activity. In this sense, there exists evidence that the antifreeze activity enhances with increasing the area/length of the ice-binding sites. In order to interpret this thermal hysteresis behavior, we introduce a two-dimensional adsorption model based on fractional statistics theory. The analytical expressions are obtained in terms of an exclusion parameter, which depend on the structure of the protein and area of the ice-binding sites. By using the model, thermal hysteresis activity is calculated for AFPs of different size, shape and number of active sites. The theoretical results show a good qualitative agreement with reported experimental data in the literature.

Key words: Equilibrium thermodynamics and statistical mechanics, Lattice-gas models, Fractional statistics theory, Thermal hysteresis activity, Antifreeze proteins

¹ Corresponding author: A. J. Ramirez-Pastor. E-mail: antorami@unsl.edu.ar

1 Introduction

It is known that some living organisms (fish, arthropods, plants, bacteria and fungi) survive in environments at very low temperatures due to the presence of a special type of protein [1–6]. Such proteins are structurally diverse. Among them, it can be mentioned one type of antifreeze glycoprotein and four different types of antifreeze proteins (AFPs): i) the type I AFP, a α -helical structure with high content of alanine, ii) the cysteine-rich type II AFP, iii) the compositionally unbiased globular protein type III AFP, and iv) an analogous to apolipoproteins of plasma called type IV AFP [7, 8].

Antifreeze proteins have the ability to lower the water freezing point, but without changing its melting point, avoiding thus ice growth by mean of the adsorption on its surface [9]. In fact, by binding to the surfaces of embryonic crystals of ice, AFPs prevent the crystal growth and, accordingly, the solution's freezing point is reduced below the melting point. Then, a thermal hysteresis (denoted as ΔT) can be defined as the difference between the melting and freezing temperatures. This quantity is a measure of the antifreeze protein activity [10, 11]. In addition, the growth of the ice crystals is inhibited in this range of temperatures and living organisms are saved from freezing.

In this context, the study of the adsorption of AFPs, and their consequent effects on the ice growth, constitutes a very demanding problem in both experimental and theoretical analysis. Among the experimental papers on antifreeze activity, the study of Baardsnes et al. [12] is of specific interest. The authors investigated the thermal hysteresis activity of a recombinant type III AFP dimer (called wlwAFP) modeled on the RD3 isoform, in comparison with that of the HPLC-12 monomer, and with that of a partially inactivated dimer (called wlxAFP) in which one of its active sites was eliminated. The obtained results revealed that the thermal hysteresis activity enhances when the area (number) of the ice-binding sites is increased. A similar effect was reported by DeLuca et al. [13], who reported that an increment in the AFP activity is observed when the type III AFP is linked to other proteins and thus its size is increased.

From a theoretical point of view, several models have been proposed relating thermal hysteresis activity with the portion of ice surface occupied by AFPs [14–29]. These approaches stimulate the researchers to develop more refined theoretical solutions for the adsorption thermodynamics of complex adsorbates (in this case, proteins of different sizes and shapes). Among them, a modified Langmuir model was proposed for studying the equilibrium adsorption of one-, two- and three-domain AFPs on the ice surface [20, 21]. A strong dependence of the activity on the protein size (number of binding domains) was found, being the activity of the three-domain protein significantly higher than the corresponding ones to one and two-domain AFPs.

The Langmuir model was improved in Ref.[22]. Each AFP molecule was modeled as a linear chain of n beads (domains) joined by flexible linkers, able to adsorb in different configurations or adsorption states. This new scheme,

denoted as lattice-gas model of molecules with multiple adsorption states, has demonstrated to be a more accurate approach to characterize the adsorption process of two- [23] and three-domain [24] AFPs. The study in Refs. [22–24] confirmed also the importance of the size and structure of the protein in determining its activity. These findings are consistent with previous results addressing the effect of impurities on the growth of crystals from aqueous solutions [25]. There it was found that the mechanism of crystal growth varies with the impurity size.

McGhee and von Hippel proposed a theoretical model to describe the adsorption of large adsorbates on a homogeneous lattice in one dimension [26]. More recently, and by generalization of the McGhee and von Hippel's theory, a model of antifreeze protein-ice adsorption was presented by Liu and Li [27]. By using the argument of Burcham et al. [14], which states that the thermal hysteresis activity varies linearly with the portion of ice surface occupied by AFPs ($\Delta T \propto \theta$), an analytical expression for ΔT was formulated as a function of protein size and adsorption constant. The model, developed in two dimensions, was applied to investigate the activity of types I [27] and III [28] AFPs.

Also following the argument of Burcham et al. [14], an adsorption kinetic model to describe thermal hysteresis activity in AFPs was presented in Ref. [29]. The model, obtained from a combinatorial approach considering multisite occupancy adsorption in two dimensions, was used to analyze two types of structurally repetitive AFPs: *Tenebrio molitor* and *Choristoneura fumiferana*. The obtained results confirm that the thermal hysteresis phenomenon depends strongly on the size of the ice-binding area (or number of ice-binding sites).

In line with previous work [14, 27–29], a model in two dimensions to study the adsorption of AFPs of different shapes and sizes on ice substrates is introduced in the present article. The theoretical scheme is based on the fractional statistics formalism [30–32]. The corresponding thermodynamic functions are analytically developed. The adsorption isotherm (fraction of sites covered by AFPs θ versus the concentration of the protein in the solution C) is expressed in terms of an exclusion parameter g , which accounts for the structure of the protein adsorption state and, accordingly, for the area of the ice-binding sites. Thus, a simple description is obtained, relating the physical properties of the system to the parameters of the theoretical approach.

To evaluate the predictive capacities of the model, two types of protein structures were considered: extended and compact (or globular) proteins. Each size-structure is characterized by a value of the exclusion parameter g . The theory reproduces the main features observed in real systems, in particular, the experimental finding showing that protein activity enhances by increasing the area/length of the ice-binding sites. Theoretical data were also used to fit thermal hysteresis experimental results of ice-binding proteins of different sizes and number of active domains [33]. Fractional theory showed to be an useful tool to interpret experimental measurements.

This work is ordered in the following way: the basis of the fractional statistics thermodynamic theory of adsorption are presented in Appendix A. In Sec. 2,

the thermal hysteresis phenomenon and its dependence on the shape/size of the adsorbed protein is investigated for extended and compact proteins. In addition, the fractional theory is used to fit and interpret experimental data of thermal hysteresis activity of *Tenebrio molitor* AFP (TmAFP) [33]. The conclusions are drawn in Sec. 3.

2 Thermal hysteresis activity of antifreeze proteins: a theoretical model based on fractional statistics thermodynamic theory of adsorption

2.1 Theoretical predictions

It is well-known that different types of AFPs inhibit the growth of ice using different mechanisms. Thus, as shown in Ref. [11], hyperactive AFPs bind to all crystal planes and the corresponding TH activity depends on the surface coverage. On the other hand, moderate AFPs cannot bind to all crystal planes (only bind to prism and/or pyramidal planes), and the resulting TH activity is independent of the surface coverage. This was also demonstrated in Ref. [11].

The model developed in the present work is restricted to the case of AFPs that bind and cover all crystal planes and their TH activity correlates with surface coverage. In this framework, and by following the ideas in Refs. [14, 27–29], the thermal hysteresis activity ΔT can be written in terms of the portion of ice surface occupied by AFP molecules Θ . Namely,

$$\frac{\Delta T}{\Delta T_m} = \frac{\Theta}{\Theta_m}, \quad (1)$$

where Θ_m and ΔT_m represent the maximum values observed of Θ and ΔT , respectively (ΔT_m corresponding to Θ_m).

According to Appendix A, the ratio Θ/Θ_m can be expressed as the fraction of ice surface occupied by AFP molecules $\theta = \Theta/\Theta_m$ [Eq. (A.20)], and θ can be calculated on the base of the fractional statistics thermodynamic theory of adsorption [30–32]. Fractional approximation provides a general theoretical scheme to model the adsorption of structured molecules. In the following, this framework will be used to study the adsorption of AFPs on ice crystals, with special emphasis on the associated thermal hysteresis phenomenon and its dependence on the shape and size of the adsorbed molecules.

In our analysis of thermal hysteresis activity, Eq. (A.20) will be used assuming that: (i) an oligomeric structure of the protein is considered, in which each protein unit is represented as a monomer²; (ii) the proteins are adsorbed in such a way that each monomer occupies one single binding site on the ice

² Molecules formed by k elemental units (called as k -mers in Appendix A) represent oligomeric proteins consisting of k monomers.

surface and double site occupancy is not allowed; (iii) the monomer-substrate adsorption energy is assumed to be constant. Phenomena such as partial unfolding or other conformational changes that may affect monomer interactions are not considered here; (iv) p is replaced by the protein solution concentration C . This allows us to address the problem of adsorption from a liquid solution; and (v) g is assumed to be constant ($g = \text{const}$). For a molecule adsorbing on the surface at zero density, there exist m available states per lattice site. Then, if the molecule occupies k' sites when adsorbed on the surface, the exclusion parameter can be written as $g = mk'$. Accordingly, $a = 1/(mk') = 1/g$ and Eq. (A.20) is as follows:

$$K(T)C = \frac{\theta [1 - \theta(g - 1)/g]^{g-1}}{g(1 - \theta)^g}. \quad (2)$$

Using Eq. (1), with $\theta = \Theta/\Theta_m$ obtained from Eq. (2), the effects of protein structure (size and shape) on the relative thermal hysteresis activity $\Delta T/\Delta T_m$ will be analyzed below.

We consider now the case of linear oligomers of k units adsorbed flat on a lattice with connectivity c . This system is characterized by $k = k'$, $m = c/2$ and $g = ck/2$. Figure 1(a) shows the relative thermal hysteresis activity in terms of the concentration of the protein in the solution for linear proteins of different sizes ($k = 1 - 4$) adsorbed on square lattices with $\beta U_0 = \beta k \epsilon_0$, being ϵ_0 the adsorption energy of each protein's unit. The curves were obtained for $\beta \epsilon_0 = -0.5$ ($\beta \epsilon_0 < 0$ corresponds to attractive adsorption energy). At a fixed value of concentration, the protein activity increases with the size.

A similar scenario is observed in the case of more compact proteins. This situation is shown in Fig. 1(b), where $\Delta T/\Delta T_m$ vs C has been calculated for $l \times l$ proteins (l^2 -mers) adsorbed flat on square lattices. Four sizes were considered: $l = 1$ (circles); $l = 2$ (squares); $l = 3$ (triangles) and $l = 4$ (diamonds). The curves were obtained by using Eqs. (1) and (2) with $g = l^2$, $c = 4$ and $\beta \epsilon_0 = -0.5$.

At $C = 0.1$, relative thermal hysteresis activity was $\Delta T/\Delta T_m \approx 0.140, 0.403, 0.530$ and 0.617 for $k = 1$ (monomers), $k = 2$ (dimers), $k = 3$ (trimers) and $k = 4$ (tetramers), respectively [see Fig. 1(a)]. The corresponding values for compact proteins were $\Delta T/\Delta T_m \approx 0.140, 0.559, 0.804$ and 0.893 for monomers ($l = 1$), 2^2 -mers, 3^2 -mers and 4^2 -mers, respectively [see Fig. 1(b)]. Clearly, antifreeze activity increases with protein size and ice-binding area (number of ice-binding sites per molecule).

The results presented in Fig. 1 demonstrate that the number of ice-binding sites per molecule plays a crucial role in the antifreeze abilities of the proteins. This finding confirms previous experimental work [33]. In Ref. [33], the TH activity of a series of structurally repetitive *Tenebrio molitor* AFPs was investigated. The authors made use of the extreme regularity of these proteins to show systematically the strong dependence of the antifreeze activity on the area of the ice-binding sites. The results are in agreement with previous data

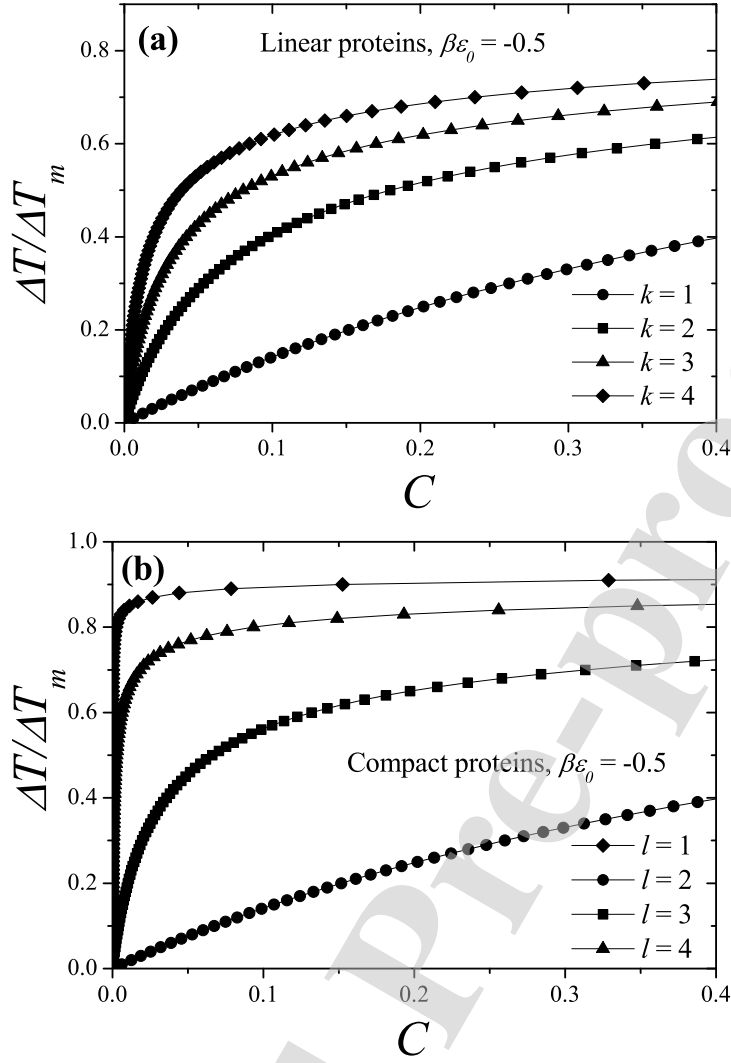


Fig. 1. Relative thermal hysteresis activity $\Delta T/\Delta T_m$ as function of the concentration of the protein in the solution C for different systems. (a) Linear proteins of different sizes adsorbed on square lattices: spherical symmetric $k = 1$ (monomers), circles; $k = 2$ (dimers), squares; $k = 3$ (trimers), triangles and $k = 4$ (tetramers), diamonds. The curves were obtained by using Eqs. (1) and (2) with $g = ck/2$, $c = 4$ (square lattices), $\beta U_0 = \beta k\epsilon_0$ and $\beta\epsilon_0 = -0.5$. (b) Compact $l \times l$ proteins of different sizes adsorbed flat on square lattices: $l = 1$ (circles); $l = 2$ (squares); $l = 3$ (triangles) and $l = 4$ (diamonds). The curves were obtained by using Eqs. (1) and (2) with $g = l^2$, $c = 4$ and $\beta\epsilon_0 = -0.5$.

from the literature [13], where it was shown that increasing the size of AFP by fusion to other proteins enhanced its activity.

The effect of inactivating domains in the AFP can be incorporated in the theory by considering heteronuclear proteins. For this purpose, let's assume that a heteronuclear protein of size k consists of s type of elements, each

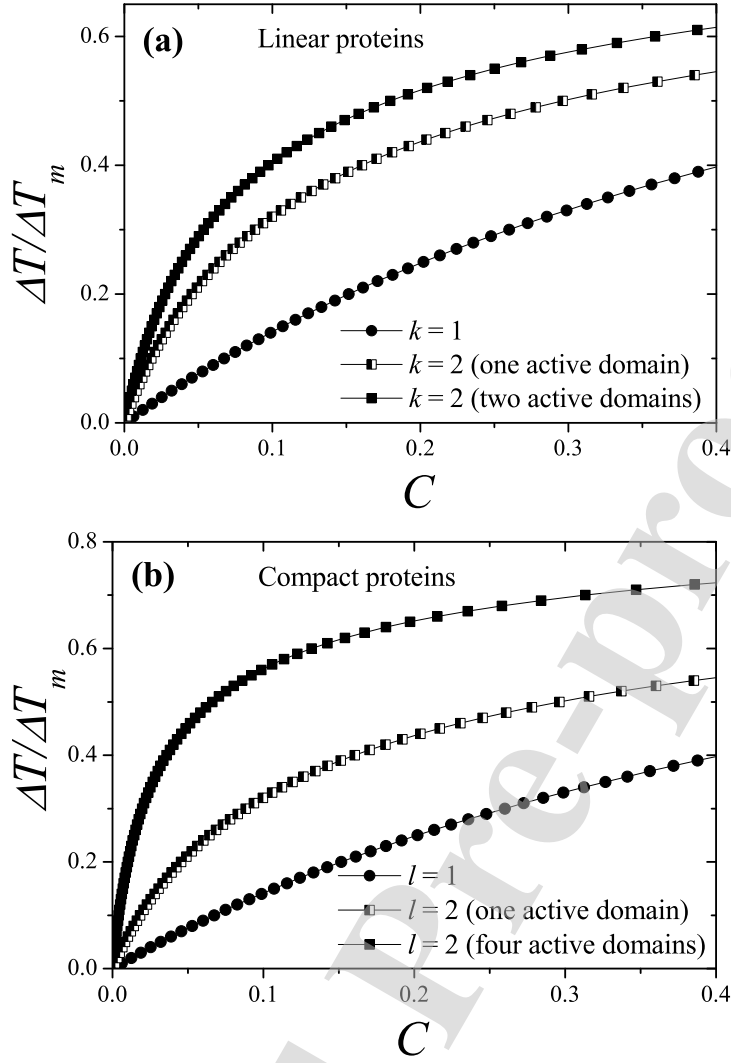


Fig. 2. Relative thermal hysteresis activity $\Delta T/\Delta T_m$ as function of the concentration of the protein in the solution C . (a) Case I (linear proteins): solid circles represent spherical symmetric monomers ($g = 1$ and $\beta U_0 = \beta \epsilon_{01} = -0.5$); solid squares correspond to homonuclear dimers ($g = ck/2 = 4$ and $\beta U_0 = 2\beta \epsilon_{01} = -1$); and semi-solid squares represent heteronuclear dimers with one active domain ($\epsilon_{01} = -0.5$) and one inactive domain ($\epsilon_{02} = 0$). Thus, $g = ck/2 = 4$ and $\beta U_0 = \beta(\epsilon_{01} + \epsilon_{02}) = -0.5$. (b) Case II (compact proteins): solid circles represent spherical symmetric monomers ($g = 1$ and $\beta U_0 = \beta \epsilon_{01} = -0.5$); solid squares correspond to homonuclear 2^2 -mers ($g = l^2 = 4$ and $\beta U_0 = 4\beta \epsilon_{01} = -2$); and semi-solid squares represent heteronuclear 2^2 -mers with one active domain ($\epsilon_{01} = -1$) and three inactive domains ($\epsilon_{02} = 0$). Thus, $g = l^2 = 4$ and $\beta U_0 = \beta(\epsilon_{01} + 3\epsilon_{02}) = -0.5$.

element or unit adsorbing individually on one lattice site. Then

$$k = \sum_{j=1}^s k_j, \quad (3)$$

where k_j is the number of j units in the protein molecule. Accordingly, the total adsorption energy of a protein constituted by s type of units is

$$U_0 = \sum_{j=1}^s k_j \epsilon_{0j}, \quad (4)$$

being ϵ_{0j} the adsorption energy between a lattice site and a group of j th type. In Fig. 2, the effect of inactivating domains in the AFP has been theoretically studied for extended (linear oligomers of k units) and compact (l^2 -mers) molecules, respectively. Square lattices ($c = 4$) were considered as substrate. Three particular adsorbates were analyzed in each case. Namely,

- Case I, Fig. 2(a): (i) solid circles, spherical symmetric monomers ($g = 1$ and $\beta U_0 = \beta \epsilon_{01} = -0.5$); (ii) solid squares, homonuclear dimers ($g = ck/2 = 4$ and $\beta U_0 = 2\beta \epsilon_{01} = -1$); and (iii) semi-solid squares, heteronuclear dimers with one active domain ($\epsilon_{01} = -0.5$) and one inactive domain ($\epsilon_{02} = 0$). Thus, $g = ck/2 = 4$ and $\beta U_0 = \beta(\epsilon_{01} + \epsilon_{02}) = -0.5$.
- Case II, Fig. 2(b): (i) solid circles, spherical symmetric monomers ($g = 1$ and $\beta U_0 = \beta \epsilon_{01} = -0.5$); (ii) solid squares, homonuclear 2^2 -mers ($g = l^2 = 4$ and $\beta U_0 = 4\beta \epsilon_{01} = -2$); and (iii) semi-solid squares, heteronuclear 2^2 -mers with one active domain ($\epsilon_{01} = -1$) and three inactive domains ($\epsilon_{02} = 0$). Thus, $g = l^2 = 4$ and $\beta U_0 = \beta(\epsilon_{01} + 3\epsilon_{02}) = -0.5$.

The data in Fig. 2 reproduce the tendency observed in the experiments: the activity curve corresponding to the protein with inactive domains remains between the curves of the monomer and the fully active protein.

The study in Figs. 1-2 shows that the parameter g has an explicit physical meaning, relating to the ice-binding area: $g \propto k$ for linear oligomers, and $g = l^2$ for compact ($l \times l$)-mers. In other words, the analytical expressions obtained from the present formalism explicitly include the dependence of the thermal hysteresis activity on the ice-binding area. This is an essential feature of our model, and allows us to interpret the thermal hysteresis behavior observed experimentally for increasing the size of the AFPs. In the next section, Eq. (2) will be applied to model experimental data of antifreeze protein activity.

2.2 Analysis of experimental data

To complete our study on the applicability of the model presented here, analysis of experimental results will be carried out in the following. The experimental data were taken from the work by Marshall et al. [33]. In Ref. [33], a hyperactive antifreeze protein from the beetle *Tenebrio molitor* (TmAFP) was investigated.

The TmAFP is a right-handed β -helix comprised of 12-amino acid repeats that stack to form a rectangular “box” with an array of Thr residues on the surface [37, 38]. In Ref. [39], it was demonstrated that the distance between Thr residues in the array matches the spacing of oxygen atoms in the ice lattice, and the Thr array is the ice-binding face of the protein. Considering the

Protein	g	$\Delta T_m(^{\circ}\text{C})$	K
TmAFP minus one coil	36	3.763	0.124
wild – type Tm 4 – 9	48	5.787	0.904
TmAFP plus one coil	72	8.224	0.911

Table 1

Theoretical parameters used for the comparison with the experimental data in Fig. 3. The values of the statistical exclusion parameter g were fixed by following the analysis in Ref. [29]. The values of ΔT_m and K were obtained by the fitting procedure discussed in the text.

extreme regularity of these AFPs, Marshall et al. [33] studied the dependence of antifreeze activity on the area of the ice-binding sites. Each of the 12-amino acid contains disulfide-bonded central coils of the TmAFP a ThrX_nThr (X_n stands for other aminoacids) ice binding motif. By means of addition and removal of coils from the parent antifreeze protein, the authors built a series of constructs with 6-11 coils.

In Ref. [33], the experiments of TH activity as a function of concentration showed that the activity of TmAFP constructs changes dramatically with the number of coils. Thus, the repetitive structure of TmAFP provides an ideal opportunity to investigate the relationship between the size and the activity of an AFP. By taking advantage of this property, we will apply our model to three different TmAFPs, which are labeled with increasing size as minus one, wild-type 4-9 (natural protein) and plus one. Interested readers are referred to Ref. [33] for a more complete description of the procedure to build Tm 4-9 AFPs of different sizes.

Before starting the comparison between experiments and theory, and given that the experimental data were informed in terms of absolute values of thermal hysteresis [ΔT ($^{\circ}\text{C}$)], it is convenient to write Eq. (1) in a more appropriate form,

$$\Delta T = \theta \Delta T_m, \quad (5)$$

where θ is obtained from Eq. (2).

The fitting procedure is as follows. First, as in Ref. [29], a square lattice is chosen as substrate ($c = 4$). This choice is arbitrary and could be replaced by any other geometry. Second, the values of g are set according to the protein structure. This structure is determined by following the arguments in Ref. [29]: TmAFP minus one coil, 6×3 rectangle with two available orientations on the lattice, $k = 18$, $m = 2$ and $g = 36$; wild-type Tm 4-9, 8×3 rectangle with two available orientations on the lattice, $k = 24$, $m = 2$ and $g = 48$; and TmAFP plus one coil, 12×3 rectangle with two available orientations on the lattice, $k = 36$, $m = 2$ and $g = 72$.

Third, minus one, wild-type and plus one experimental points are simultaneously fitted by using Eq. (5) [with θ obtained from Eq. (2)] and a least-squares

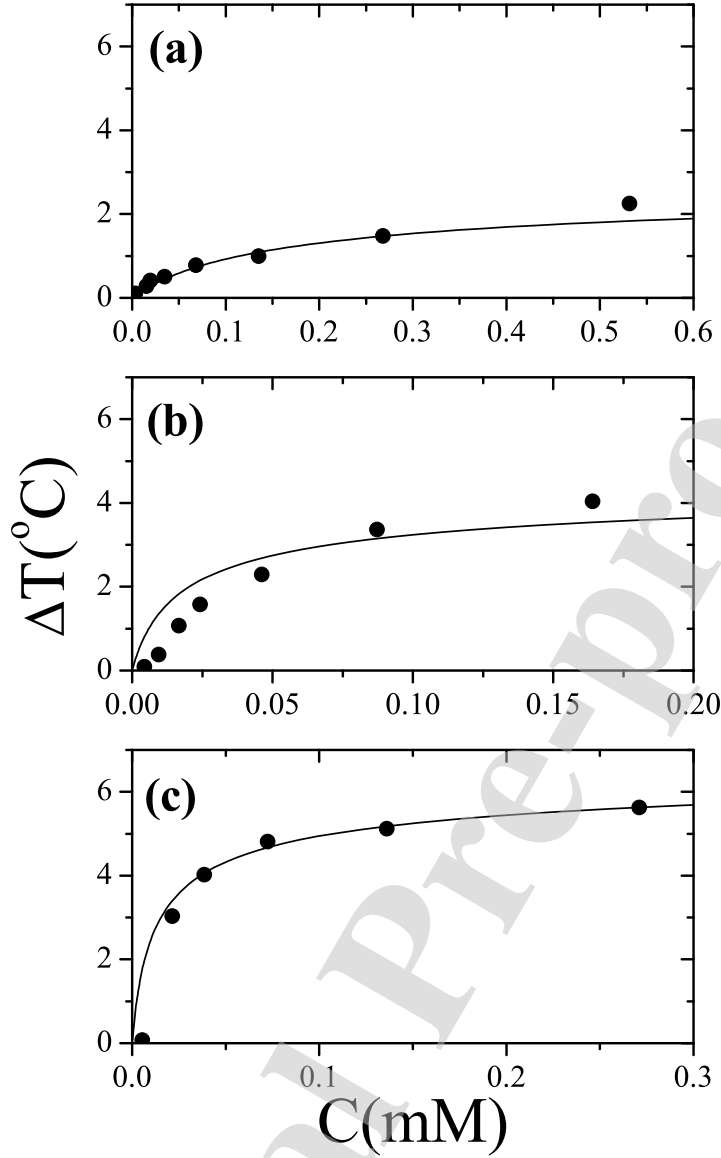


Fig. 3. Curves of thermal hysteresis activity for TmAFP minus one coil (a), wild-type Tm 4-9 (b), and TmAFP plus one coil (c). Symbols represent data from Ref. [33], and solid lines correspond to analytical results from Eqs. (2) and (5). The parameters obtained from the fitting procedure are: $\Delta T_m = 3.763$ $^{\circ}\text{C}$ and $K = 0.124$ (TmAFP minus one coil); $\Delta T_m = 5.787$ $^{\circ}\text{C}$ and $K = 0.904$ (wild-type Tm 4-9); and $\Delta T_m = 8.224$ $^{\circ}\text{C}$ and $K = 0.911$ (TmAFP plus one coil).

procedure [40]. Thus, n experimental points $(x_i, y_i, z_i; i = 1, \dots, n)$ are adjusted to an analytical function with L fitting parameters $(a_j; j = 1, \dots, L)$. The following functionality between dependent and independent variables is predicted by the model,

$$z(x, y) \equiv z(x, y; a_1 \dots a_L), \quad (6)$$

where the right-hand side of Eq. (6) indicates explicitly the dependence on the fitting parameters. Then, as it is standard in this type of problems, the parameters are adjusted to achieve a minimum in the function,

$$\sum_{i=1}^n [z_i - z(x_i, y_i; a_1 \dots a_L)]^2, \quad (7)$$

yielding best-fit parameters.

The adjustment procedure was carried out for the complete set of experimental data. The function $z(x, y) \equiv z(x, y; a_1 \dots a_L)$ was obtained from Eq. (5), with ΔT_m and K as fitting parameters for each studied protein. The obtained results are presented in Fig. 3: (a) TmAFP minus one coil; (b) wild-type Tm 4-9 and (c) TmAFP plus one coil. The values of the fitting parameters are compiled in Table 1. Solid lines correspond to theoretical data and symbols represent experimental results from Ref. [33].

A good qualitative agreement is observed between theoretical and experimental data. In order to better rationalize these differences, it is convenient to define the relative ($\varepsilon_{r,i}$) errors for each point i in the curves of thermal hysteresis activity,

$$\varepsilon_{r,i} = \left| \frac{\Delta T_i^{\text{theo}} - \Delta T_i^{\text{exp}}}{\Delta T_i^{\text{exp}}} \right|_{C_i}, \quad (8)$$

where ΔT_i^{exp} (ΔT_i^{theo}) indicates the thermal hysteresis activity calculated from experiments (theoretical approximation). Each pair ($\Delta T_i^{\text{exp}}, \Delta T_i^{\text{theo}}$) is calculated at fixed C_i .

It is also useful to define a percentage average relative error for each thermal hysteresis curve,

$$E_r(\%) = \left(\frac{\sum_i^n \varepsilon_{r,i}}{n} \right) \times 100\%, \quad (9)$$

which accounts for the differences between experimental and theoretical results in all range of concentration. n is the number of experimental points in the thermal hysteresis activity curve.

In Fig. 3, the obtained values of the percentage average relative errors were: $E_r(\%) = 18.6\%$ (TmAFP minus one coil, $n = 8$ points); $E_r(\%) = 28.4\%$ (wild-type Tm 4-9, $n = 7$ points); and $E_r(\%) = 3.2\%$ (TmAFP plus one coil, $n = 5$ points). In the case of wild-type Tm 4-9 and TmAFP plus one coil, the experimental points corresponding to the lowest concentration (with ΔT of the order of 10^{-3}) were discarded for the error analysis.

The obtained values of the quantity K , which account for the protein-ice adsorption energy, are consistent with previous findings in Ref. [29], where the number of effective (active) adsorption sites n_a was informed. n_a is the same for wild-type Tm 4-9 and TmAFP plus one coil, and changes for TmAFP minus one coil. Accordingly, the values of K obtained from the fitting procedure are practically the same for the cases in Figs. 3(b) and 3(c). A different value is obtained in the case of Fig. 3(a).

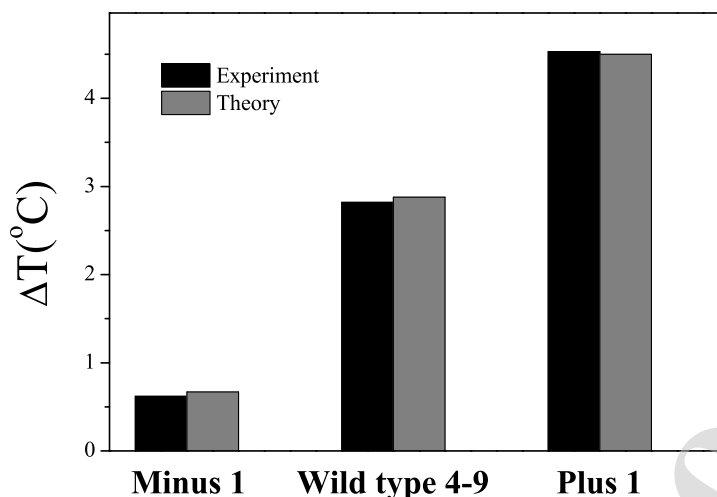


Fig. 4. Comparison of the theoretically predicted ΔT and the corresponding experimental values of the studied TmAFP constructs at a protein concentration of $60 \mu\text{M}$. Dark and gray bars represent experimental (reproduced from Ref. [33]) and theoretical results, respectively.

With respect to ΔT_m , the resulting values increase with the size of the protein. A similar effect is presented in Fig. 4. The figure shows ΔT at a protein concentration of $60 \mu\text{M}$ (the gray bars represent the values obtained from the model, and the dark bars correspond to experimental results reproduced from Ref. [33]). Clearly, the thermal hysteresis activity increases with protein size and ice-binding area.

To conclude with the analysis of Fig. 3, it is important to mention that the simplest relationship between thermal hysteresis activity and surface coverage has been used here, assuming that $\Delta T \propto \theta$. As shown in Ref. [21], alternative mathematical expressions ($\Delta T \propto \theta^{1/2}$ and $\Delta T \propto \theta^n$, being n an adjustable parameter) could be used to analyze the experimental data. In addition, several authors have pointed out that kinetic models of the type presented by Kubota [41] are a better representation in the case of moderate proteins like those studied in Fig. 3 [42]. Covering these topics in depth is out of scope for this article. However, the analysis carried out in this section confirms and strengthens the conclusions of previous analyses [29, 27, 28, 13, 12]. Namely, the thermal hysteresis activity enhances with increasing the area/length of the ice-binding sites.

3 Conclusions

In this paper, a theoretical model to study antifreeze protein adsorption to ice and thermal hysteresis activity has been presented. The new scheme combines (i) the argument of Burcham et al. [14], which indicates that the thermal hysteresis activity depends linearly on the fraction of ice surface occupied by AFPs; and (ii) the fractional theory of adsorption [31, 32], where the struc-

ture of the adsorbed species is explicitly considered. The model addresses hyperactive AFPs, which bind and cover all crystal planes. The resulting description allows us to write the thermal hysteresis activity as a function of a statistical exclusion parameter, g , which takes into account the configuration of the protein in the adsorbed state and number of ice-binding sites (effective adsorption area per molecule).

Two types of proteins were considered to investigate the thermal hysteresis phenomenon and its dependence on the shape and size of the adsorbate: extended and compact proteins, modeled as linear oligomers of k units and $l \times l$ square tiles, respectively. The theory reproduces the main features observed in real systems, in particular, the experimental finding that antifreeze activity increases with increasing the effective adsorption area (length) per molecule, being $g \propto k$ and $g = l^2$ for linear and compact proteins, respectively.

The theoretical predictions were compared with experimental data from Ref. [33], where thermal hysteresis activity of ice-binding proteins of different sizes and number of active domains was investigated. The cases of TmAFP minus one coil, wild-type Tm 4-9 and TmAFP plus one coil were studied in detail. A good fitting of the experimental data was obtained, validating the conjecture that the effective adsorption area per molecule is the main factor governing the protein activity.

The theoretical framework introduced here provides an useful tool for understanding and interpreting the phenomenon of protein-ice adsorption, showing that, the differences in activity are the result of the difference of the number of ice-binding sites between the adsorbed molecules. In this way, lattice geometry and adsorbate configuration play important roles in determining the thermodynamics and function of the adsorbed proteins.

Classical adsorption models, generally obtained by simple modifications of the Langmuir model [35], retain the original assumption that each adsorbed molecule occupies one surface site. In this approach, the spatial arrangement of the adsorption sites is immaterial, and accordingly, these theoretical models do not distinguish the different structures of the adsorption states. As an example, in Refs. [20, 21], a simple modified Langmuir model was developed to study the adsorption of two- and three-domain AFPs on ice. The dependence of the thermal hysteresis activity on the protein surface coverage was investigated. However, the limitations of the approximation did not allow to investigate the effect of the protein structure (size/shape/compactness).

It is important to note that different values of the adsorption constants (or adsorption energies) would be necessary to interpret thermal hysteresis data of AFPs of different sizes in the framework of a Langmuir model. Clearly, it is a fictitious way of taking into account steric or geometric effects by means of energetic arguments. In other words, a real interpretation of the thermal hysteresis phenomenon requires that the effect of the adsorbate structure be adequately incorporated into the theory.

On the other hand, theoretical approximations based on the counting of configurations in finite lattices have proved to be a useful tool to investigate the

thermal hysteresis activity problem [29, 27, 28]. In Refs. [29, 27, 28], a two-dimensional model of AFP-ice adsorption was introduced. In this framework, the ice surface was modeled using M chains and N adsorption sites on each chain. In addition, it was assumed that the AFP molecule can occupy any $m \times n$ adjacent sites on the ice surface. By using a computer code written in C++, the authors calculated the surface coverage as a function of the size parameters M , N , m and n , showing that precise results can be obtained if $\min(M, N) > 30 \max(m, n)$.

It is clear that the complete AFP-ice adsorption problem is far from being solved. The structural diversity of the antifreeze proteins in the adsorbed state still constitutes a major difficulty to obtain theoretical expressions for the adsorption thermodynamic functions. These considerations, along with the arguments given in the last three paragraphs, stimulate the development of analytical formalisms suitable for describing the problem of structured species with multiple adsorption states. The model developed in this paper represents a step in this direction, providing an important improvement with respect to previous models on protein-ice adsorption. Thus, a complete thermodynamic scheme of compact equations was presented. The theory was developed in the framework of the rigorous statistical mechanics of infinite systems ($N, M \rightarrow \infty$) [34], providing close analytical solutions for the thermodynamic functions. These solutions can be easily extended to other lattice geometries and protein structures. The concept of statistical exclusion was properly considered, allowing to manage the complex entropic contribution of structured adsorbates through the parameter g .

Finally, it is important to note that more sophisticated protein adsorption systems can be investigated on the basis of the present model. Among them, deserve to be mentioned: (i) systems in the presence of multilayer adsorption ($g < 1$); (ii) systems that present configurational transitions in the adlayer when the surface coverage is varied. In this case, the statistical exclusion can be described by a function depending on the density $g(\theta)$; and (iii) complex systems, where the adsorption states are correlated in space, and multiple exclusion statistics must be considered (see Ref. [32]).

4 ACKNOWLEDGMENTS

The authors thank Prof. Peter L. Davies and Prof. Rodolfo Porasso for useful discussion and suggestions. This work was supported in part by CONICET (Argentina) under project number PIP 112-201701-00673CO; Universidad Nacional de San Luis (Argentina) under projects 03-0816 and 02-2116; and the National Agency of Scientific and Technological Promotion (Argentina) under project PICT-2013-1678. The numerical work were done using the BACO parallel cluster (http://cluster_infap.unsl.edu.ar/wordpress/) located at Instituto de Física Aplicada, Universidad Nacional de San Luis - CONICET, San Luis, Argentina.

A Fractional statistics thermodynamic theory of adsorption

A.1 Basic formalism: adsorption thermodynamic functions

Let's assume $(N - 1)$ identical particles within a fixed volume V containing G equilibrium states of energy $E(N)$. The number of states available to the N^{th} particle when added to the volume is

$$d_N = G - \sum_{N'=1}^{N-1} g(N') = G - G_0(N). \quad (\text{A.1})$$

Equation (A.1) represents a generalization of the Pauli exclusion principle, and is the basis of the Haldane statistics [30]. In Ref. [31], the Haldane statistics was extended to treat multisite-occupancy adsorption. The resulting approximation, called fractional statistic thermodynamic theory of adsorption, assumes that the interaction of a solid substrate with one isolated molecule can be modeled by an adsorption field with G local minima in the coordinate space. Thus, G can be thought of as the total number of available states for a single molecule. In the case of lattice-gas models, the adsorption field is represented by an array of adsorption sites (lattice). Since the particles are supposed to be identical, d_N is the total number of available states to the N particles confined in V . Then, the number of configurations of a system of G states and N molecules is

$$W(N) = \frac{(d_N + N - 1)!}{[N!(d_N - 1)!]} = \frac{[G - G_0(N) + N - 1]!}{\{N![G - G_0(N) - 1]!\}}, \quad (\text{A.2})$$

which follows from the number of distinguishable permutations. As it can be observed from Eq. (A.1), Bose and Fermi statistics are recovered in the limits $g(N) = 0$ (no exclusion at all) and $g(N) = 1$ (each particle excludes one state), respectively: $W(N) = (G + N - 1)!/[N!(G - N)!]$ for $g(N) = 0$; and $W(N) = G!/[N!(G - N)!]$ for $g(N) = 1$.

The Helmholtz free energy $F(N, T, V)$ is

$$\beta F(N, T, V) = -\ln Q(N, T, V), \quad (\text{A.3})$$

where $\beta = 1/k_B T$ with k_B being the Boltzmann constant, and the canonical partition function, $Q(N, T, V)$, is

$$Q(N, T, V) = W(N) \exp[-\beta E'(N)]. \quad (\text{A.4})$$

$E'(N)$ involves all interactions present in the system of N particles (although we assume here it only to depend on N). Thus, $E'(N) = E_i(N) + E(N)$, where $E_i(N)$ corresponds to the energy of the internal degrees of freedom of the isolated particle and $E(N)$ the energy involving all remaining interactions

(adsorption energy and adsorbate-adsorbate lateral interactions). Accordingly,

$$Q(N, T, V) = W(N)q_i^N \exp[-\beta E(N)] \quad (\text{A.5})$$

where q_i is the partition function of one isolated particle. We observe also that G is proportional to V , thus $G = \tilde{a}V$, being \tilde{a} the number of equilibrium states (adsorption minima) per unit of volume. Using the Stirling's approximation for $\ln x! = x \ln x - x$ in $\ln W(N)$,

$$\begin{aligned} \ln Q(N, T, V) &= [\tilde{a}V - G_0(N) + N - 1] \ln [\tilde{a}V - G_0(N) + N - 1] \\ &\quad - [\tilde{a}V - G_0(N) - 1] \ln [\tilde{a}V - G_0(N) - 1] \\ &\quad - N \ln N + N \ln q_i - \beta E(N) \end{aligned} \quad (\text{A.6})$$

and

$$\begin{aligned} \frac{\beta F(N, T, V)}{V} &= -\frac{1}{V} \{ [\tilde{a}V - G_0(N) + N - 1] \ln [\tilde{a}V - G_0(N) + N - 1] \\ &\quad - [\tilde{a}V - G_0(N) - 1] \ln [\tilde{a}V - G_0(N) - 1] \\ &\quad - N \ln N + N \ln q_i - \beta E(N) \}. \end{aligned} \quad (\text{A.7})$$

Let us continue by defining the free energy density $\tilde{f}(\rho) = \lim_{N,V \rightarrow \infty} \frac{F}{V}$, $\tilde{G}_0(\rho) = \lim_{N,V \rightarrow \infty} \frac{G_0(N)}{V}$ and $\tilde{\epsilon}(\rho) = \lim_{N,V \rightarrow \infty} \frac{E(N)}{V}$, being $\rho = \frac{N}{V}$. Then,

$$\begin{aligned} \beta \tilde{f}(\rho, T) &= -\{ [\tilde{a} - \tilde{G}_0(\rho) + \rho] \ln [\tilde{a} - \tilde{G}_0(\rho) + \rho] \\ &\quad - [\tilde{a} - \tilde{G}_0(\rho)] \ln [\tilde{a} - \tilde{G}_0(\rho)] \\ &\quad - \rho \ln \rho + \rho \ln q_i - \beta \tilde{\epsilon}(\rho) \}. \end{aligned} \quad (\text{A.8})$$

The chemical potential can be obtained from $\mu = \left(\frac{\partial F}{\partial N} \right)_{T,V} = \left(\frac{\partial \tilde{f}}{\partial \rho} \right)_T$ [34]

$$\begin{aligned} \beta \mu &= -[\tilde{G}_0'(\rho) - 1] \ln [\tilde{a} - \tilde{G}_0(\rho) + \rho] \\ &\quad - \tilde{G}_0'(\rho) \ln [\tilde{a} - \tilde{G}_0(\rho)] + \ln \rho - \ln q_i + \beta \tilde{\epsilon}'(\rho), \end{aligned} \quad (\text{A.9})$$

where $\tilde{G}_0'(\rho) = \frac{\partial \tilde{G}_0(\rho)}{\partial \rho}$ and $\tilde{\epsilon}'(\rho) = \frac{\partial \tilde{\epsilon}(\rho)}{\partial \rho}$. Then, the general expression for the adsorption isotherm in the proposed description arises

$$\exp(\beta \mu) = \frac{\exp[\beta \tilde{\epsilon}'(\rho)] \rho [\tilde{a} - \tilde{G}_0(\rho) + \rho]^{\tilde{G}_0'(\rho)-1}}{q_i [\tilde{a} - \tilde{G}_0(\rho)]^{\tilde{G}_0'(\rho)}}. \quad (\text{A.10})$$

The entropy density $\tilde{s} = S/V$ can also be obtained from Eq. (A.8) and the following relationship [34]:

$$\tilde{s} = \frac{S}{V} = -\frac{1}{V} \left(\frac{\partial F}{\partial T} \right)_{N,V} = -\left(\frac{\partial \tilde{f}}{\partial T} \right)_\rho. \quad (\text{A.11})$$

Thus,

$$\begin{aligned} \frac{\tilde{s}(\rho, T)}{k_B} = & \{\rho \ln q_i + [\tilde{a} - \tilde{G}_0(\rho) + \rho] \ln [\tilde{a} - \tilde{G}_0(\rho) + \rho] \\ & - [\tilde{a} - \tilde{G}_0(\rho)] \ln [\tilde{a} - \tilde{G}_0(\rho)] - \rho \ln \rho\}. \end{aligned} \quad (\text{A.12})$$

A.2 Thermodynamic functions for lattice-like systems

In order to apply the derived thermodynamic functions to a lattice-like adsorption system, we consider that the substrate is represented by a regular lattice of M “adsorption sites”. For spherical particles which only occupy an adsorption site it is clear that the total number of accessible states to a single particle equals M ($G = M$). However, for structured particles (particles composed by many units like polyatomics) this one-to-one correspondence between adsorption site \rightarrow adsorption state is no longer valid. Note the multiple configurations that a single molecule can adopt on the surface having a unit occupying an adsorption site. In general $G > M$ from this point of view.

Thus, it is convenient to define an adimensional density $n = N/G$ so that $n = N/(V\tilde{a}) = \rho/\tilde{a}$. By replacing it in Eq. (A.8), and defining $f(n, T) = \tilde{f}(n/\tilde{a}, T)/\tilde{a}$, it results

$$\begin{aligned} \beta f(n, T) = & -\{[1 - \Gamma_0(n) + n] \ln [1 - \Gamma_0(n) + n] \\ & - [1 - \Gamma_0(n)] \ln [1 - \Gamma_0(n)] \\ & - n \ln n + n \ln q_i - \beta \epsilon(n)\}, \end{aligned} \quad (\text{A.13})$$

where

$$\Gamma_0(n) = \frac{\tilde{G}_0(\rho)}{\tilde{a}} = \lim_{V, N \rightarrow \infty; N/V\tilde{a}=n} \frac{G_0(N)}{V\tilde{a}} \quad (\text{A.14})$$

and

$$\epsilon(n) = \frac{\tilde{\epsilon}(n\tilde{a})}{\tilde{a}} = \lim_{V, N \rightarrow \infty; N/V\tilde{a}=n} \frac{E(N)}{V\tilde{a}}. \quad (\text{A.15})$$

The resulting adsorption isotherm equation can be written as:

$$\exp(\beta\mu) = \frac{\exp[\beta\epsilon'(n)] n [1 - \Gamma_0(n) + n]^{\Gamma_0'(n)-1}}{q_i [1 - \Gamma_0(n)]^{\Gamma_0'(n)}}. \quad (\text{A.16})$$

The adimensional density n can be straightforward related to the standard definition of relative surface coverage θ , through

$$n = \frac{N}{G} = a \frac{N}{N_m} = a \frac{V}{V_m} = a\theta, \quad (\text{A.17})$$

where N_m (V_m) represents the total number of particles (total volume) adsorbed on a full monolayer. From Eq. (A.17), it comes that $a^{-1} = G/N_m \equiv$ number of equilibrium states per particle; so related directly to the characteristics of the adsorption field and the shape/size of the adsorbed molecules.

It is straightforward the relationship between the quantities \tilde{a} and a introduced before. $V\tilde{a} = G = N_m/a \Rightarrow \tilde{a} = N_m/aV = a^{-1}\rho_m$, ρ_m being the maximum density of the adsorbed phase. Replacing Eq. (A.17) in Eq. (A.16),

$$\exp(\beta\mu) = \frac{\exp[\beta\epsilon'(a\theta)]}{q_i} \frac{a\theta [1 - \Gamma_0(a\theta) + a\theta]^{\Gamma'_0(a\theta)-1}}{[1 - \Gamma_0(a\theta)]^{\Gamma'_0(a\theta)}}. \quad (\text{A.18})$$

Equation A.19 can also be written as a function of the surface coverage θ :

$$\frac{s(a\theta)}{k_B} = \{(a\theta) \ln q_i + [1 - \Gamma_0(a\theta) + a\theta] \ln [1 - \Gamma_0(a\theta) + a\theta] - [1 - \Gamma_0(a\theta)] \ln [1 - \Gamma_0(a\theta)] - (a\theta) \ln(a\theta)\}, \quad (\text{A.19})$$

where $s(a\theta) = s(n) = \tilde{s}(n/\tilde{a})/\tilde{a}$.

From the general expression of the adsorption isotherm given in Eq. (A.18), we will address a number of special cases of adsorption of model polyatomics in order to analyze the predictions of the theory for various adsorption configurations, molecular shapes and sizes, etc.

A.3 Lowest approximation of the fractional theory: $g = \text{constant}$. Adsorption of molecules of different sizes and shapes

We now analyze the simplest approach, in the framework of the fractional theory, which takes into account the statistical (entropic) effects of molecular configuration in the adsorption isotherm, namely, $g = \text{constant}$. Thus, $\Gamma_0(n) = gn$, $\Gamma'_0(n) = g$ and $\epsilon'(n) = U_0$, where U_0 is the adsorption energy per particle. The adsorption isotherm equation results,

$$K(T)p = \frac{a\theta [1 - a\theta(g-1)]^{g-1}}{(1 - a\theta g)^g}, \quad (\text{A.20})$$

where $p \propto \exp(\beta\mu)$ is the pressure and $K(T)$ is the adsorption constant $K(T) = q_i \exp(-\beta U_0)$. For simplicity, the partition function of one isolated particle is set equal to one ($q_i = 1$), without any loss of generality.

The parameters g and a in Eq. (A.20) can be derived from experimental measurements, and provide valuable information regarding the spatial configuration of the adsorbed molecules. On the other hand, Eq. (A.20) can be applied by modeling g in terms of the model parameters. Then, given the lattice structure and size/shape of the adsorbate, the adsorption thermodynamic functions are straightforwardly obtained.

The fractional formalism is mathematically manageable, and allows us to incorporate in the model the entropic contribution arising from the spatial structure of complex adsorbates. Some examples of such complex adsorbates will be discussed below.

Let us consider molecules formed by elemental units deposited on an array of M adsorption sites and c connectivity, such that k' out of k units are attached

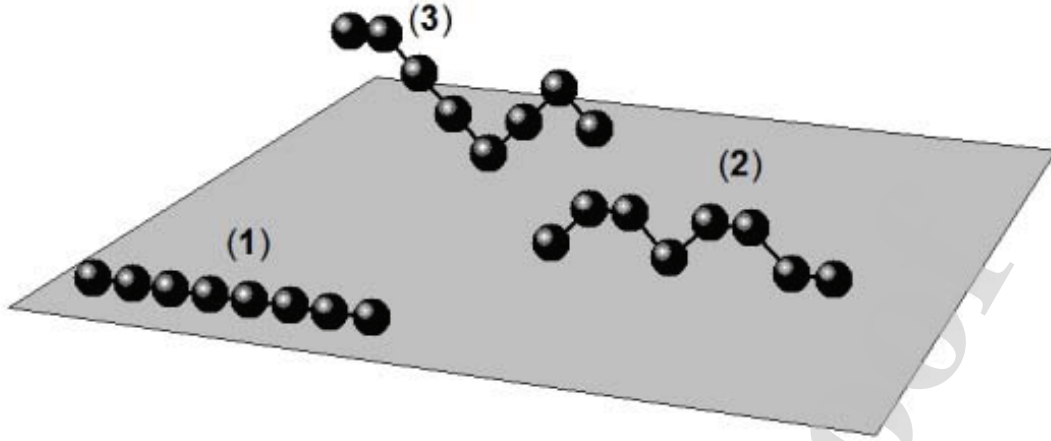


Fig. A.1. Schematic diagram showing three different available configurations corresponding to a chain of 8 units adsorbed on a planar surface: (1) $k = k' = 8$; (2) $k = 8$ and $k' = 4$; and (3) $k = 8$ and $k' = 1$.

to the surface sites and $(k - k')$ detached from the surface and tilted away from it (see Fig. A.1).

After the definition Eq. (A.17), the surface coverage will then be $\theta = N/N_m = N/(M/k') = k'N/M$. The total number of equilibrium states is $G = mM$, being m the number of distinguishable states corresponding to a single molecule per lattice site (at $\theta \rightarrow 0$). Hence, from $a^{-1} = G/N_m = nM/(M/k') = mk'$ (it should be addressed that m is a measure “per site” and a is “per molecule”).

For instance, for spherical symmetric monomers adsorbed on a lattice $k = k' = 1$, $m = 1$ and $a = 1$. Thus, by taking $g = 1$, Eq. (A.20) reduces to the Langmuir adsorption isotherm equation [35]. For a straight molecule of k units adsorbed horizontally on a one-dimensional chain $k = k'$, $m = 1$ and $a = 1/k$. In addition, if $g = k$, the use of Eq. (A.20) leads to the rigorous exact expression of the adsorption isotherm corresponding to the case of linear k -mers adsorbed horizontally on a one-dimensional chain [36].

The examples above allow us to propose an interpretation of the exclusion parameter g . Let us start from the definition $\Gamma_0(n) = gn$ and analyze the limit cases $\Gamma_0(0) = 0$ and $\Gamma_0(n_m) = 1$, where $n_m = N_m/G$. Then, $\Gamma_0(n_m) = gN_m/G = 1$ and, consequently, $g = G/n_m = 1/a$. This explains the choice of $g = 1$ and $g = k$ for monomers and k -mers on one-dimensional lattices, respectively.

As other examples of application, $k = k'$, $m = 2$, $a = 1/2k$ and $g = 2k$ correspond to straight rigid k -mers deposited horizontally on square lattices. Finally, $m = 1$, $a = 1/k'$ and $g = k'$ represent the one-dimensional adsorption of k -mers with k' units attached to the substrate and $(k - k')$ units detached and tilted with respect to the surface.

References

- [1] C.H.C. Cheng, *Curr. Opin. Genet. Dev.* 8 (1998) 715.
- [2] H.J. Kim, J.H. Lee, Y.B. Hur, C.W. Lee, S.-H. Park, B.-W. Koo, *Mar. Drugs* 15 (2017) 1.
- [3] L.A. Graham, P.L. Davies, *Science* 310 (2005) 461.
- [4] M.E. Urrutia, J.G. Duman, C.A. Knight, *Biochim. Biophys. Acta* 1121 (1992) 199.
- [5] J.A. Gilbert, P.J. Hill, C.E.R. Dodd, J. Laybourn-Parry, *Microbiology-SGM* 150 (2004) 171.
- [6] C.H. Robinson, *New Phytol.* 151 (2001) 341.
- [7] N. Pertaya, C.B. Marshall, Y. Celik, P.L. Davies, I. Braslavsky, *Biophys J.* 95 (2008) 333.
- [8] P.L. Davies, *Trends Biochem. Sci.* 39 (2014) 548.
- [9] M. Bar Dolev, I. Braslavsky, P.L. Davies, *Annu. Rev. Biochem.* 85 (2016) 515.
- [10] J. Barrett, *Int. J. Biochem. Cell Biol.* 33 (2001) 105.
- [11] R. Drori, P.L. Davies, I. Braslavsky, *RSC Adv.* 5 (2015) 7848.
- [12] J. Baardsnes, M.J. Kuiper, P.L. Davies, *J. Biol. Chem.* 278 (2003) 38942.
- [13] C.I. DeLuca, R. Comley, P.L. Davies, *Biophys. J.* 74 (1998) 1502.
- [14] T.S. Burcham, D.T. Osuga, Y.A. Yeh, *J. Boil. Chem.* 261 (1986) 6390.
- [15] S. Wang, N. Amornwittawat, X. Wen, *J. Chem. Thermodyn.* 53 (2012) 125.
- [16] H. Katsuno, K. Katsuno, M. Sato, *Phys. Rev. E* 84 (2011) 021605.
- [17] B. Kutschan, K. Morawetz, S. Thoms, *Phys. Rev. E* 90 (2014) 022711.
- [18] L.-F. Li, X.X. Liang, *Physica A* 421 (2015) 355.
- [19] Z. Dong, J. Wang, X. Zhou, *Phys. Rev. E* 95 (2017) 052140.
- [20] Ö. Can, N.B. Holland, *J. Colloid Interface Sci.* 329 (2009) 24.
- [21] Ö. Can, N.B. Holland, *Biochemistry* 52 (2013) 8745.
- [22] E. Quiroga, A.J. Ramirez-Pastor, *Chem. Phys. Lett.* 556 (2013) 330 .
- [23] C.F. Nambuena, F.O. Sanchez Varretti, A.J. Ramirez-Pastor, *Phys. Chem. Chem. Phys.* 18 (2016) 24549.
- [24] J.I. Lopez Ortiz, P. Torres, E. Quiroga, C.F. Nambuena, A.J. Ramirez-Pastor, *Phys. Chem. Chem. Phys.* 19 (2017) 31377.
- [25] N. Kubota, J.W. Mullin, *J. Cryst. Growth* 152 (1995) 203.
- [26] J.D. McGhee, P.H. von Hippel, *J. Mol. Biol.* 86 (1974) 469.
- [27] J.J. Liu, Q.Z. Li, *Chem. Phys. Lett.* 422 (2006) 67.
- [28] J. Liu, W. Xie, in *3rd International Conference on Biomedical Engineering and Informatics (BMEI 2010)*, edited by W. Yu, M. Zhang, L. Wang, Y. Song, 6 2387 (2010).
- [29] Q.Z. Li, Y. Yeh, J.J. Liu, R.E. Feeney, V.V. Krishnan, *J. Chem. Phys.* 124 (2006) 204702.
- [30] F.D.M. Haldane, *Phys. Rev. Lett.* 67 (1991) 937.
- [31] J.L. Riccardo, A.J. Ramirez-Pastor, F. Romá, *Phys. Rev. Lett.* 93 (2004) 186101.

- [32] J.J. Riccardo, J.L. Riccardo, A.J. Ramirez-Pastor, P.M. Pasinetti, *Phys. Rev. Lett.* 123 (2019) 020602.
- [33] C.B. Marshall, M.E. Daley, B.D. Sykes, P.L. Davies, *Biochemistry* 43 (2004) 11637.
- [34] T.L. Hill, *An Introduction to Statistical Thermodynamics*, Addison Wesley Publishing Company, Reading, MA, 1960.
- [35] I. Langmuir, *J. Am. Chem. Soc.* 40 (1918) 1361.
- [36] A.J. Ramirez-Pastor, T.P. Eggarter, V.D. Pereyra, J.L. Riccardo, *Phys. Rev. B* 59 (1999) 11027.
- [37] Y.C. Liou, A. Tocilj, P.L. Davies, Z. Jia, *Nature (London)* 406 (2000) 322.
- [38] M.E. Daley, L. Spyropoulos, Z. Jia, P.L. Davies, B.D. Sykes, *Biochemistry* 41 (2002) 5515.
- [39] C.B. Marshall, M.E. Daley, L.A. Graham, B.D. Sykes, P.L. Davies, *FEBS Lett.* 529 (2002) 261.
- [40] W.H. Press, S.A. Teukolsky, W.T. Vetterling, B.P. Flannery, *Numerical Recipes in C: The Art of Scientific Computing*, Cambridge University Press, New York, 1992.
- [41] N. Kubota, *Cryobiology* 63 (2011) 198.
- [42] M. Chasnitsky, I. Braslavsky, *Phil. Trans. R. Soc. A* 377 (2019) 20180391.

Thermal hysteresis activity of antifreeze proteins: a model based on fractional statistics theory of adsorption

J. I. Lopez Ortiz, E. Quiroga, C. F. Nambuena, J. L. Riccardo, A. J. Ramirez-Pastor

Highlights

> A new approach to model thermal hysteresis (TH) activity of antifreeze protein is presented. > The formalism is based on fractional statistics theory of adsorption. > An explicit dependence of the TH activity on the area of the ice-binding sites is obtained. > The theory is applied to interpret experimental data of ice-binding proteins of different sizes and number of active domains. > TH activity increases with increasing the number and area of the ice-binding sites.

REF.: CRediT author statement

Ms.: PHYSA-201483 Thermal hysteresis activity of antifreeze proteins: a model based on fractional statistics theory of adsorption, by J. I. Lopez Ortiz, E. Quiroga, C. F. Nambuena, J. L. Riccardo, A. J. Ramirez-Pastor

J. I. Lopez Ortiz: Conceptualization, Methodology, Software, Investigation. **E. Quiroga:** Conceptualization, Writing - review & editing. **C. F. Nambuena:** Conceptualization, Methodology. **J. L. Riccardo:** Conceptualization, Methodology. **Antonio J. Ramirez-Pastor:** Conceptualization, Methodology, Writing - original draft, Writing - review & editing.

Declaration of interests

The authors declare that they have no known competing financial interests or personal relationships that could have appeared to influence the work reported in this paper.

The authors declare the following financial interests/personal relationships which may be considered as potential competing interests:

Journal Pre-proof